NJC

PAPER

View Article Online
View Journal | View Issue

Cite this: *New J. Chem.*, 2016, **40**, 7018

Electronic and optical properties of 5-AVA-functionalized BN nanoclusters: a DFT study

Alireza Soltani,*[a] Ahmad Sousaraei,[a] Masoud Bezi Javan,[b] Mortaza Eskandari[c] and Hanzaleh Balakheyli[d]

Received (in Montpellier, France) 20th February 2016,
Accepted 6th June 2016

DOI: 10.1039/c6nj00146g

www.rsc.org/njc

We carried out detailed density functional theory (DFT) and time-dependent density functional theory (TD-DFT) calculations upon 5-aminolevulinic acid-functionalized $B_{12}N_{12}$ and $B_{16}N_{16}$ nanoclusters with the B3LYP, B3PW91, and PBE methods using the 6-311+G** basis set. The calculated adsorption energies of 5-aminolevulinic acid with the BN nanoclusters were evaluated at T = 298.15 and 311.15 K in the gaseous and aqueous environments with the B3LYP, B3PW91, and PBE methods. Our results showed that the adsorption of the 5-AVA molecule (NH_2 group) with $B_{12}N_{12}$ is more favorable than – with the $B_{16}N_{16}$ nanocluster in the gas and solvent phases. It is anticipated that a 5-aminolevulinic acid (5-AVA) drug incorporating BN clusters could find application in drug delivery systems and in biomedical devices.

1. Introduction

Bioconjugated nanostructured materials have become visible as novel materials for medical diagnostics and biosensing applications in recent years,[1,2] for example, pristine BN nanostructures are recognized as promising candidates for such applications. Boron nitride nanotubes (BNNTs), a morphologically similar prototype of carbon nanotubes (CNTs) with different properties of their own, for instance with the capabilities of uniformity and stability in dispersion in solution, are known as particularly promising candidates for biomedical applications.[3–6] Their electronic structures and properties vary widely owing to the tube helicity and concentric layers, unlike CNTs, and their semiconducting properties, regardless of their diameter and chirality, which make these materials suitable for electronic applications.[7,8] BNNTs are renowned as nontoxic materials to health and the environment owing to their chemical inertness and structural stability, and hence, they are useful in the development of drug delivery systems, novel biosensors, biofunctional materials, nanovectors for cell therapy, and gene delivery studies.[9–13] Within the hemechromophore in the mitochondria is a compound called 5-aminolevulinic acid (5-AVA), which is considered to be a key synthetic building block in protoporphyrin IX (PpIX). Under the negative feedback control mechanism of heme, ALA could be synthesized in mitochondria. Basically, the mechanism is initiated by the building of glycine and succinyl CoA, with this being catalyzed *via* ALA-syntase, making this the first intermediate synthesizing agent that undergoes a series of biochemical reactions. Consequently, in the presence of iron, PpIX is converted into heme by ferrochelatase. A great deal of attention has been paid to the inclination of 5-ALA for inducing protoporphyrin IX (PpIX) in tumor cells after its exogenous administration. It has been used to detect and/or facilitate the photodestruction of malignant tissue and in the preoperative delineation of malignant brain tumors due to its fluorescence and photosensitizing properties, which can help lengthen patient survival.[14,15] The recent strategies in PDT (photodynamic therapy) for patients include prescribing 5-ALA and/or alkyl esters, through one of three approaches, namely by direct injection into the tissue, by administration in the blood, or by topical application to the skin.[16,17] Recently, a broad variety of investigations has been performed upon the electrical and structural properties of pure and functionalized 5-ALA. For instance, Eriksson and Erdtman carried out a theoretical study of 5-aminolevulinic acid and some pharmaceutically important derivatives.[14] Ganji *et al.* carried out a DFT study on the interaction of the $B_{36}N_{36}$ cluster with glycine amino acid.[18] Gou and co-workers[19] performed DFT calculations to investigate the noncovalent functionalization of BN nanotubes with perylene derivative molecules. Xie *et al.* experimentally found that BN nanotubes can be functionalized with amino-based systems. Regarding the noncovalent functionalizations of BNNTs by aromatic compounds, surfactants, and polymers, π–π stacking interactions have drawn increasing attention due to their potential applications in upgrading novel biosensors, and as biofunctional materials, nanovectors for cell therapy, and in

[a] *Young Researchers and Elite Club, Gorgan Branch, Islamic Azad University, Gorgan, Iran. E-mail: Alireza.soltani46@yahoo.com, g.chem1983@gmail.com; Tel: +98-938-4544921*
[b] *Physics Department, Faculty of Sciences, Golestan University, Gorgan, Iran*
[c] *Department of Chemistry, Institute for Advanced Studies in Basic Sciences, Gavazang, Zanjan, Iran*
[d] *Joints, bones and connective tissue research center, Golestan University of Medical Science, Gorgan, Iran*

drug and gene delivery systems.[20] Zhao and Ding used theoretical calculations to investigate the interaction of the noncovalent functionalization of BN nanotubes by various aromatic molecules.[21] Zhi *et al.* studied how BN nanotubes could be noncovalently functionalized by wrapping them with DNA.[22] Very recently, Ciofani *et al.* experimentally investigated how BN nanotubes could be coated by polyethyleneimine (PEI), indicating the essential stipulations for the biomedical applications of BN nanotubes.[12] In previous theoretical work,[23] we performed the interaction of 5-ALA drug with carbon nanostructures using DFT calculations. Herein, we aimed to consider the electronic and structural properties of 5-ALA functioned with $B_{12}N_{12}$ and $B_{16}N_{16}$ nanoclusters to further understand $B_{12}N_{12}$ and $B_{16}N_{16}$ capacity for use in drug delivery applications.

2. Computational methods

Geometry optimizations, density of states (DOS), frontier molecular orbital (FMO), and natural bond orbital (NBO) analyses were performed with the GAMESS quantum chemistry software package.[24] All the calculations were based on the density functional theory (DFT) and time-dependent density functional theory (TD-DFT) with the B3LYP method with the standard 6-311+G** basis set.[25] B3LYP is indicated to be a dependable and usually applied functional in the study of different BN nanostructures.[26–28] We utilized the exchange–correlation functional parameterized by PBE and B3PW91 with superposition error (BSSE) correction.[29,30] In the PCM calculations, water was used as a solvent, with a value of ε = 78.4 for the dielectric constant. Adsorption calculations were carried out in gaseous and aqueous environments at T = 298.15 and 310.15 K. After optimization, the obtained B–N bond length of $B_{12}N_{12}$ was found to be about 1.486, 1.493, and 1.492 Å, and are 1.473, 1.481, and 1.480 Å in a 4-cycle for the $B_{16}N_{16}$ cage with the B3LYP, PBE, and B3PW91 methods, respectively (see Table 1). The adsorption energies (E_{ad}) of 5-AVA on the pure BN nanocages are represented by:

$$E_{ad} = E_{cage-molecule} - (E_{cage} + E_{molecule}) + E_{BSSE} \quad (1)$$

where E_{cage} is the adsorption energies of the pristine $B_{12}N_{12}$ and $B_{16}N_{16}$ nanocages. $E_{cage-molecule}$ is the adsorption energy of 5-AVA interacting with the pristine $B_{12}N_{12}$ and $B_{16}N_{16}$ clusters, and $E_{molecule}$ represents the energy of an isolated 5-AVA molecule. The quantum molecular descriptors[31,32] for the nanocage were determined as follows:

$$\mu = -(I + A)/2 \quad (2)$$

$$\chi = -\mu \quad (3)$$

$$\eta = (I - A)/2 \quad (4)$$

$$S = 1/2\eta \quad (5)$$

$$\omega = (\mu^2/2\eta) \quad (6)$$

The electronegativity (χ) is defined as the negative of the chemical potential (μ), as follows: $\chi = -\mu$. Furthermore, the global hardness (η) can be determined using the Koopmans' theorem. $I(-E_{HOMO})$ is the ionization potential and $A(-E_{LUMO})$ is the electron affinity of the molecule.

3. Results and discussion

Initially, we computationally optimized the geometry of an individual 5-aminolevulinic acid molecule (5-AVA) within the gas phase; see Fig. 1 and Table 2. All the nitrogen and oxygen atoms form essentially a planar structure with carbon atoms implying sp^2 orbital hybridization, thus maintaining the aromatic characteristics. Fig. 1a–c indicate the molecular electrostatic potential (MEP), the highest occupied molecular orbital (HOMO), and the lowest unoccupied molecular orbital (LUMO) of a 5-aminolevulinic acid molecule. It is apparent that the electron densities in the HOMO and LUMO are situated on the amine and carbonyl orbitals of the molecule and on the CH_2 group. The energy gap (E_g) and Fermi level (E_F) of the 5-aminolevulinic acid molecule are 2.21 and −3.57 eV with the B3LYP method, respectively. This result reveals that the 5-aminolevulinic

Table 1 Calculated structural and electronic properties of the $B_{12}N_{12}$ and $B_{16}N_{16}$ nanocages with the B3PW91, B3LYP, and PBE methods

	B3LYP		B3PW91		PBE	
System	$B_{12}N_{12}$	$B_{16}N_{16}$	$B_{12}N_{12}$	$B_{16}N_{16}$	$B_{12}N_{12}$	$B_{16}N_{16}$
R_{B-N}/Å	1.486	1.473	1.485	1.471	1.494	1.481
R_{B-N-B}/°	80.50	78.53	80.12	78.15	79.95	77.85
R_{N-B-N}/°	98.23	99.34	98.44	99.56	98.58	99.81
R_{N-B-N}/°						
Q_B/e	0.450	0.44	0.459	0.482	0.387	0.389
Q_N/e	−0.450	−0.44	−0.459	−0.482	−0.387	−0.390
E_{HOMO}/eV	−7.85	−7.38	−7.98	−7.56	−6.91	−6.49
E_{LUMO}/eV	−1.11	−1.01	−1.05	−1.10	−1.92	−1.88
E_g/eV	6.74	6.37	6.93	6.46	4.99	4.61
E_{FL}/eV	−4.48	−4.20	−4.52	−4.33	−4.42	−4.19
μ/eV	−4.48	−4.19	−4.52	−4.33	−4.42	−4.19
η/eV	3.37	3.19	3.47	3.23	2.50	2.31
ω/eV	2.98	2.76	2.94	2.90	3.91	3.80
S/eV	0.15	0.16	0.14	0.15	0.20	0.22
χ/eV	4.48	4.19	4.52	4.33	4.42	4.19
D_M/Debye	0.00	0.0	0.0	0.0	0.0	0.0

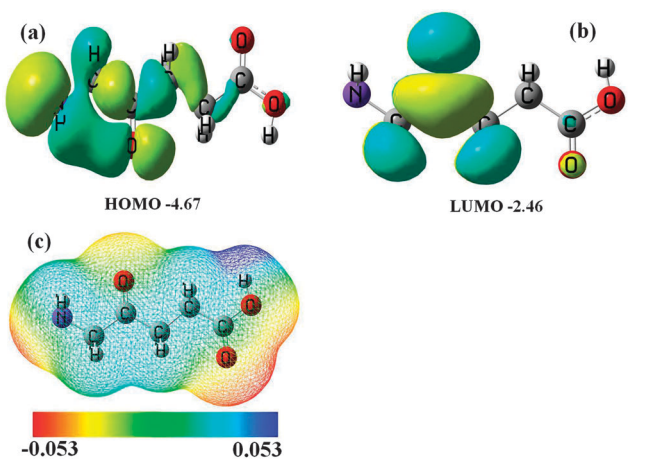

Fig. 1 The profiles of HOMO (a), LUMO (b), and MEP (c) of 5-aminolevulinic acid with the B3LYP method.

Table 2 Results obtained from geometry optimizations of the 5-aminolevulinic acid molecule in the B3LYP method

System	R_{C-N}/Å	R_{C-H}/Å	R_{C-O}/Å	R_{O-H}/Å	R_{C-C-C}/°	R_{C-C-N}/°	$R_{N-C-C-C}$/°	$R_{C-C-C-C}$/°
R_{B-N}/Å	1.452	1.095	1.212	0.964	116.6	116.1	179.6	179.5

acid molecule with a large energy gap is a hard molecule.[31] Also, the dipole moment (D_M) of this drug molecule is about 2.27 Debye. The relaxed geometries of the 5-AVA–$B_{12}N_{12}$ and 5-AVA–$B_{16}N_{16}$ systems with the B3LYP method are shown in Fig. 2A–C and 3A–C. To evaluate the preferred interaction, the interaction of the 5-AVA drug with the boron atoms of the $B_{12}N_{12}$ and $B_{16}N_{16}$ clusters was studied. The chemisorption energy of the 5-AVA molecule from its $-NH_2$ group close to the $B_{12}N_{12}$ and $B_{16}N_{16}$ clusters was calculated to be −1.33 and −1.20 eV, respectively (see Table 3).

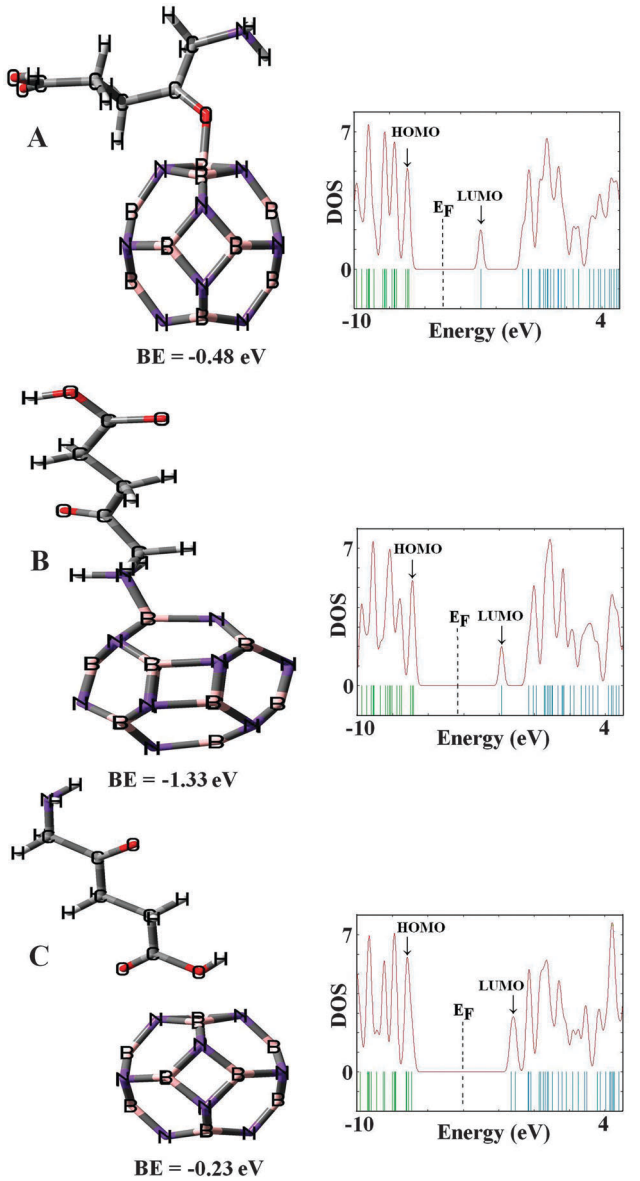

Fig. 2 Optimized structures and the electronic density of states of 5-aminolevulinic acid over the $B_{12}N_{12}$ nanocage.

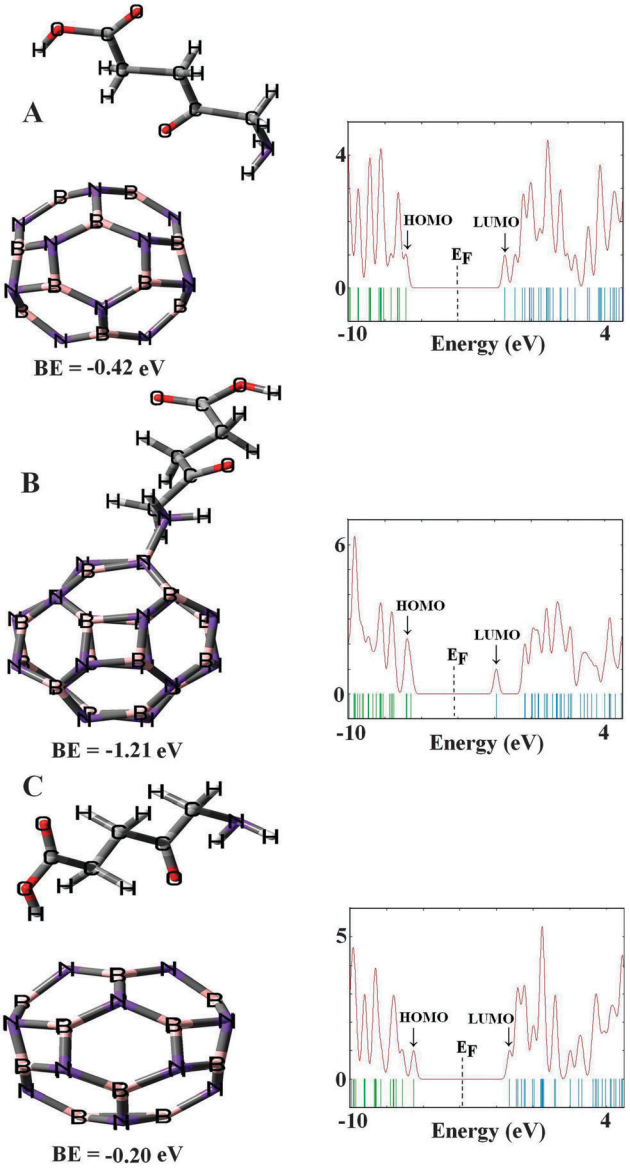

Fig. 3 Optimized structures and the electronic density of states of 5-aminolevulinic acid over the $B_{16}N_{16}$ nanocage.

The distances of the drug molecule with the NH_2 group attached to the B atoms of the $B_{12}N_{12}$ and $B_{16}N_{16}$ nanoclusters are 1.629 and 1.638 Å, respectively. NBO reveals that notable charge transfers occurred of 0.337 and 0.274 electrons from the 5-AVA molecule as a donor to the $B_{12}N_{12}$ and $B_{16}N_{16}$ nanoclusters. We noted that the interaction of 5-AVA drug on the $B_{12}N_{12}$ cluster has the largest adsorption energy, while the interaction of this drug molecule with the $B_{16}N_{16}$ nanocluster is the smallest (see Fig. 3A–C).

Table 3 Calculated structural and electronic properties of 5-aminolevulinic acid molecule interacting with the $B_{12}N_{12}$ and $B_{16}N_{16}$ nanocages in the B3LYP method

System	NH_2/$B_{12}N_{12}$	CO/$B_{12}N_{12}$	OH/$B_{12}N_{12}$	NH_2/$B_{16}N_{16}$	CO/$B_{16}N_{16}$	OH/$B_{16}N_{16}$
R_{B-N}/Å	1.515	1.548	1.539	1.553	1.488	1.486
R_{B-N-B}/°	83.80	84.35	82.45	82.13	79.34	78.10
R_{N-B-N}/°	92.15	92.40	94.29	93.15	98.20	99.12
R_{N-B-N}/°						
R_{NH_2}/Å	1.023	1.018	1.019	1.023	1.019	1.020
R_{CO}/Å	1.218	1.244	1.218	1.218	1.224	1.220
R_{OH}/Å	0.972	0.972	0.980	0.972	0.972	0.981
D/Å	1.629	1.616	1.822	1.638	2.310	2.016
E_{ad}/eV	−1.33	−0.48	−0.23	−1.20	−0.42	−0.20
Q_B/e	0.628	0.621	0.601	0.652	0.558	0.499
Q_N/e	−0.515	−0.545	−0.524	−0.510	−0.491	−0.552
Q_{NH_2-AVA}/e	−0.693	−0.681	−0.682	−0.710	−0.704	−0.684
Q_{CO-AVA}/e	−0.446	−0.387	−0.394	−0.446	−0.433	−0.457
Q_{OH-AVA}/e	−0.561	−0.557	−0.610	−0.561	−0.567	−0.614
E_{HOMO}/eV	−6.84	−6.93	−6.91	−6.59	−6.85	−6.53
E_{LUMO}/eV	−1.86	−2.86	−1.28	−1.91	−1.44	−1.29
E_g/eV	4.98	4.07	5.63	4.68	5.41	5.24
ΔE_g (%)	−27.20	40.58	−17.69	−26.5	−20.91	−23.39
E_{FL}/eV	−4.35	−4.90	−4.10	−4.25	−4.15	−3.91
μ/eV	−4.35	−4.90	−4.10	−4.25	−4.15	3.91
η/eV	2.49	2.04	2.82	2.34	2.71	2.62
ω/eV	3.80	5.89	2.98	3.86	3.18	2.92
S/eV	0.20	0.25	0.18	0.21	0.18	0.19
χ/eV	4.35	4.90	4.10	4.25	4.15	3.91
D_M/Debye	7.67	6.57	5.66	7.40	1.197	3.99

Table 4 Calculated structural and electronic properties of the 5-aminolevulinic acid molecule interacting with the $B_{12}N_{12}$ and $B_{16}N_{16}$ nanocages in the B3PW91 and PBE methods

	B3PW91			PBE		
System	NH_2/$B_{12}N_{12}$	CO/$B_{12}N_{12}$	OH/$B_{12}N_{12}$	NH_2/$B_{12}N_{12}$	CO/$B_{12}N_{12}$	OH/$B_{12}N_{12}$
R_{B-N}/Å	1.566	1.545	1.541	1.576	1.575	1.552
R_{B-N-B}/°	83.37	84.17	82.89	83.39	84.20	82.15
R_{N-B-N}/°	92.24	92.58	94.20	92.29	92.57	94.32
R_{NH_2}/Å	1.021	1.014	1.015	1.032	1.023	1.025
R_{CO}/Å	1.210	1.237	1.209	1.223	1.252	1.222
R_{OH}/Å	0.963	0.963	0.970	0.974	0.975	0.981
D/Å	1.617	1.613	1.775	1.630	1.622	1.797
E_{ad}/eV	−1.39	−0.51	−0.23	−1.49	−0.63	−0.32
Q_B/e	0.548	0.524	0.563	0.472	0.432	0.471
Q_N/e	−0.398	−0.430	−0.409	−0.347	−0.375	−0.361
Q_{N-AVA}/e	−0.385	−0.439	−0.442	−0.362	−0.408	−0.414
Q_{CO-AVA}/e	−0.310	−0.237	−0.310	−0.271	−0.191	−0.265
Q_{OH-AVA}/e	−0.303	−0.299	−0.375	−0.263	−0.260	−0.321
E_{SOMO}/eV	−7.15	−7.22	−7.14	−6.08	−6.17	−5.91
E_{LUMO}/eV	−2.01	−2.98	−1.49	−2.96	−3.85	−2.42
E_g/eV	5.14	4.24	5.66	3.12	2.32	3.49
ΔE_g (%)	−25.83	−38.82	−18.33	−37.47	−53.51	−30.06
E_{FL}/eV	−4.58	−5.10	−4.32	−4.52	−5.01	−4.17
μ/eV	−4.58	−5.10	−4.32	−4.52	−5.01	−4.17
η/eV	2.57	2.12	2.83	1.56	1.16	1.75
ω/eV	4.08	6.13	3.30	6.55	10.82	4.97
S/eV	0.19	0.24	0.18	0.32	0.43	0.29
χ/eV	4.58	5.10	4.32	4.52	5.01	4.17
D_M/Debye	7.48	6.47	6.02	7.48	6.45	6.70

Then, we compared the present studies with the adsorption of the 5-AVA molecule to the pristine carbon nanostructures in the previous reports.[23] The calculated binding energy of the 5-AVA molecule in the active sites, including NH_2 and CO groups interacting with the C_{24} nanocage, is about −0.79 and −0.89 eV, with the B3LYP method, respectively. Based on this research, the interaction energy of the 5-AVA molecule with the carbon nanocage is significantly unstable in terms of its active sites in comparison with that of the BN nanocages. Based on the acquired results, the B–N bond length and N–B–N angle of the 5-AVA/$B_{12}N_{12}$ complex were found to be 1.564 Å and 92.15°, while for the 5-AVA/$B_{16}N_{16}$ complex the same were 1.569 Å and 93.15°, respectively. Upon the interaction, the N–H bond length and H–N–H angle of the 5-AVA molecule are 1.024 Å and 105.02°, respectively. The bond lengths of C–N and C–O in the pure 5-AVA molecule are 1.453 and 1.219 Å with the B3LYP method, respectively. Erdtman and Eriksson[14] showed that the C–N and C–O lengths of the 5-AVA molecule are about 1.457 and 1.226 Å at the B3LYP/6-31+G* level, respectively, which is comparable with our results. The calculated binding energies of the 5-AVA molecule from its −OH group with the two systems, including the $B_{12}N_{12}$ and $B_{16}N_{16}$ nanoclusters, are −0.23 and −0.20 eV with the distances of 1.82 and 2.01 Å, respectively. Anota and Cocoletzi[33] showed the adsorption between the metformin molecule and (5, 5) BNNT, with an energy value of −0.63 eV, which is a result of the exothermic process. We also calculated the adsorption of the 5-AVA molecule in the most stable configuration (from its NH_2 group) toward $B_{12}N_{12}$ and $B_{16}N_{16}$ clusters at the PBE functional (see Table 4). The binding energies acquired for the 5-AVA molecule (NH_2 group) on the B atoms of the $B_{12}N_{12}$ and $B_{16}N_{16}$ clusters are included with the exothermic adsorption energies of −1.49 and −1.38 eV, respectively. These are very different from the above theoretical values (with the B3LYP method). The smaller atomic distances between the N atom of the molecule and the B atoms of the $B_{12}N_{12}$ and $B_{16}N_{16}$ clusters are 1.630 and 1.638 Å, respectively. Besides, the interaction of the 5-AVA molecule with BN nanoclusters with the PBE method indicates a considerable reduction in adsorption energy compared with the B3LYP method. The N–H bond lengths in the 5-AVA molecule added to the $B_{12}N_{12}$ and $B_{16}N_{16}$ clusters were 1.036 and 1.031 Å, respectively, which are larger than the isolated 5-AVA bond length (N–H = 1.023 Å); whereas the B–N lengths of the $B_{12}N_{12}$ and $B_{16}N_{16}$ clusters after the adsorption of the 5-AVA molecule were found to be 1.576 and 1.554 Å, respectively. Therefore, we considered that the covalent interaction at the above-mentioned separation will be strong in nature. MPA reveals that notable charge transfers are occurring in terms of 0.321 and 0.320 electrons from the 5-AVA molecule to the $B_{12}N_{12}$ and $B_{16}N_{16}$ clusters with the PBE functional. These results clearly show that the charge transfer occurring for both systems are almost the same. Ganji *et al.* introduced the binding energy of a glycine molecule adsorbed upon the $B_{36}N_{36}$ cage with an energy value of −1.15 eV in the PBE method.[18] In contrast, when the 5-AVA molecule adsorbed on the $B_{12}N_{12}$ and $B_{16}N_{16}$ nanoclusters in the PBE method, it exhibited that the binding energies for both two systems were reduced with notable changes, as compared with that in B3LYP method. The adsorption energies of the isoniazid drug upon the (5, 5) and (10, 0) BN nanotubes have been reported with the values of −0.649 and −0.738 eV

with the PBE functional, respectively.[34] The adsorption energy of the 5-AVA molecule is close to that of the $B_{12}N_{12}$ nanocluster, therefore it appears to be stronger than those in the 5-AVA molecule interacting with the $B_{16}N_{16}$ nanocluster. When considering the 5-AVA molecule from its NH_2 group interaction with the B atoms of the $B_{12}N_{12}$ and $B_{16}N_{16}$ clusters, the values of the electric dipole moment are significantly increased from 0.0 Debye in the pure structures to 7.67 and 7.40 Debye in the complexes in the PBE method, respectively. As calculated by the PBE method, the dipole moment values for 5-AVA approaching the $B_{12}N_{12}$ and $B_{16}N_{16}$ nanoclusters significantly increased from zero in the pure structures to 7.48 and 7.40 Debye in the complex configurations, respectively. In other words, we consider the interaction of 5-AVA with $B_{12}N_{12}$ and $B_{16}N_{16}$ nanoclusters with the contact values of 1.623 and 1.630 Å in the B3PW91 functional. It was found that the adsorption of the 5-AVA molecule with the $B_{12}N_{12}$ and $B_{16}N_{16}$ clusters is exothermic, with the high negative values of −1.39 and −1.30 eV, respectively. The high negative E_{ad} of the 5-AVA drug on the exterior surfaces of the $B_{12}N_{12}$ and $B_{16}N_{16}$ nanoclusters indicates the chemical nature of the interaction. NBO reveals that notable charge transfers are occurring in 0.304 and 0.299 electrons from the 5-AVA molecule to the $B_{12}N_{12}$ and $B_{16}N_{16}$ nanoclusters in the B3PW91 functional. In the adsorption process between the adsorbate and adsorbent, a local structural deformation is attributed to the change from sp^2 to sp^3 hybridization of the B atom, where the sidewall boron atom is significantly pulled out of the surface (by about 0.1 Å), indicating that the interaction is mainly covalent in nature. The D_M for 5-AVA molecule close to the $B_{12}N_{12}$ and $B_{16}N_{16}$ clusters is significantly increased to 7.48 and 7.34 Debye in the B3PW91 functional, respectively (Table 4).

Fig. 4 indicates the HOMO (highest occupied molecular orbital) and LUMO (lowest unoccupied molecular orbital) profiles for the 5-AVA molecule (NH_2 group) toward the $B_{12}N_{12}$ nanocluster. These profiles represent that the HOMO orbital is mainly localized on the nanocage and the LUMO orbital is localized on the drug molecule. As shown in Fig. 4, the LUMO+1, LUMO+2, and LUMO+3 are located at the higher energy levels compared to the LUMO, while the HOMO−3 is located at the lower energy level compared to the HOMO. These profiles imply that the value of E_{ad} in HOMO–LUMO orbital interactions depends on the overlap and energy match between the mixing orbitals, and suggests that a greater energy discrepancy between the interacting HOMO and LUMO leads to higher E_{ad}.

The adsorption behavior of the 5-AVA molecule toward $B_{12}N_{12}$ nanocluster under different temperatures (from 298.15 to 311.15 K) in the gas phase was studied (Table 5). The results indicate that the adsorption energy initially decreases with increasing temperature. As a result, the highest adsorption energy can be observed at 298.15 K, and the lowest minimum adsorption energy can be obtained at 398.15 K. The adsorption energies between the 5-AVA molecule and $B_{12}N_{12}$ cluster at the temperature of 398.15 K were calculated to be −1.37, −1.45, and −1.54 eV in the B3LYP, B3PW91, and PBE methods, respectively, suggesting that the adsorption behaviors of drug molecule are exothermic processes. The different energy distribution found in adsorption behavior at 398.15 K has no effect on the distance between the drug molecule and adsorbent (1.629, 1.623, and 1.631 Å in the B3LYP, B3PW91, and PBE, respectively). Solvation energies (E_{solv}) of the pure $B_{12}N_{12}$ interacting with the 5-AVA molecule have been studied in the B3LYP,

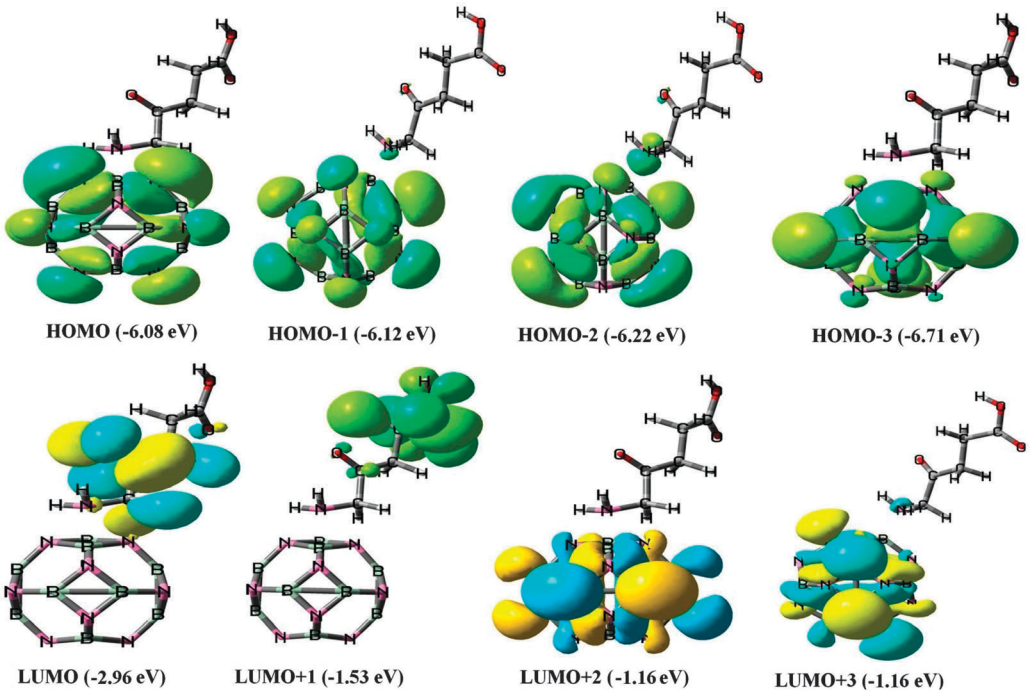

Fig. 4 Isosurfaces of HOMO and LUMO orbitals of 5-aminolevulinic acid over the $B_{16}N_{16}$ nanocage.

Table 5 Calculated structural and electronic properties of 5-aminolevulinic acid molecule interacting with the $B_{12}N_{12}$ and $B_{16}N_{16}$ nanocages at temperature of 311.15 K

	B3LYP		B3PW91		PBE	
System	$B_{12}N_{12}$	AVA/$B_{12}N_{12}$	$B_{12}N_{12}$	AVA/$B_{12}N_{12}$	$B_{12}N_{12}$	AVA/$B_{12}N_{12}$
R_{B-N}/Å	1.487	1.565	1.485	1.565	1.494	1.573
R_{B-N-B}/°	80.50	83.81	80.12	83.80	79.94	83.45
R_{N-B-N}/°	98.23	92.09	98.44	92.15	98.58	92.53
D/Å	—	1.629	—	1.629	—	1.631
E_{ad}/eV	—	−1.18	—	−1.26	—	−1.34
Q_B/e	0.440	0.631	0.459	0.629	0.387	0.532
Q_N/e	−0.440	−0.517	−0.459	−0.517	−0.387	−0.456
Q_{N-AVA}/e	—	−0.691	—	−0.696	—	−0.676
E_{HOMO}/eV	−7.71	−6.85	−7.89	−7.0	−6.78	−5.89
E_{LUMO}/eV	−0.87	−1.84	−0.90	−1.91	−1.72	−2.83
E_g/eV	6.84	5.01	6.99	5.09	5.06	3.06
ΔE_g (%)	—	−26.75	—	−27.18	—	−39.52
E_{FL}/eV	−4.29	−4.35	−4.40	−4.46	−4.25	−4.36
μ/eV	−4.29	−4.35	−4.40	−4.46	−4.25	−4.36
η/eV	3.42	2.51	3.50	2.55	2.53	1.53
ω/eV	2.69	3.77	2.76	3.90	3.57	6.21
S/eV	0.15	0.20	0.14	0.20	0.20	0.33
χ/eV	4.29	4.35	4.40	4.46	4.25	4.36
D_M/Debye	0.00	7.89	0.00	7.57	0.00	7.58

B3PW91, and PBE methods for optimizing the structures in a vacuum and in water compared to that in the gas phase (see Table 6). The difference between these optimization energies equals E_{solv}. The solvation energies were computed with the aid of the 'Conductor-like Screening Model' for solvation.[31] A more negative E_{solv} will result in a higher degree of solubility. The solvation energy values of the 5-AVA drug molecule were calculated to be −0.38, −0.39, and −0.34 eV in the B3LYP, B3PW91, and PBE methods, respectively. E_{solv} values for the 5-AVA drug with the $B_{12}N_{12}$ nanocage were about −1.42, −1.51, and −1.59 eV in the B3LYP, B3PW91, and PBE methods,

Table 6 Calculated structural and electronic properties of 5-aminolevulinic acid molecule interacting with the $B_{12}N_{12}$ and $B_{16}N_{16}$ nanocages in the solvent phase

	B3LYP (H_2O)		B3PW91 (H_2O)		PBE (H_2O)	
System	$B_{12}N_{12}$	AVA/$B_{12}N_{12}$	$B_{12}N_{12}$	AVA/$B_{12}N_{12}$	$B_{12}N_{12}$	AVA/$B_{12}N_{12}$
R_{B-N}/Å	1.486	1.578	1.484	1.574	1.494	1.583
R_{B-N-B}/°	80.54	83.96	80.11	83.62	79.95	83.63
R_{N-B-N}/°	98.18	91.24	98.46	91.60	98.60	91.64
D/Å	—	1.606	—	1.601	—	1607
E_{ad}/eV	−0.38	−1.42	−0.39	−1.51	−0.34	−1.59
Q_B/e	0.449	0.652	0.469	0.648	0.396	0.548
Q_N/e	−0.449	−0.509	−0.469	−0.522	−0.396	−0.447
Q_{N-AVA}/e	—	−0.705	—	−0.743	—	−0.685
E_{HOMO}/eV	−7.70	−6.96	−7.87	−7.12	−6.77	−6.02
E_{LUMO}/eV	−0.80	−1.07	−0.83	−1.13	−1.66	−2.11
E_g/eV	6.90	5.89	7.04	5.99	5.11	3.91
ΔE_g (%)	—	−14.64	—	−14.91	—	−23.48
E_{FL}/eV	−4.25	−4.02	−4.35	−4.13	−4.22	−4.07
μ/eV	−4.25	−4.02	−4.35	−4.13	−4.22	−4.07
η/eV	3.45	2.95	3.52	2.99	2.56	1.96
ω/eV	2.62	2.74	2.69	2.84	3.48	4.23
S/eV	0.14	0.17	0.14	0.17	0.19	0.26
χ/eV	4.25	4.02	4.35	4.13	4.22	4.07
D_M/Debye	0.00	10.26	0.00	10.27	0.00	9.72

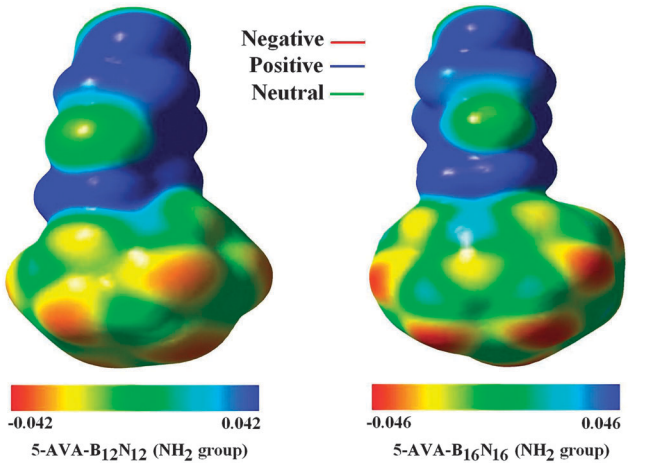

Fig. 5 The molecular electrostatic potential of 5-aminolevulinic acid molecule interacting with the $B_{12}N_{12}$ and $B_{16}N_{16}$ nanocages.

respectively. On loading 5-AVA drug molecule toward the $B_{12}N_{12}$ nanocage, E_{solv} gets a further deduction, thus showing an increase in the solubility of the drug molecule in the presence of solvent. The molecular electrostatic potential (MEP) maps for the 5-AVA molecule interacting with the $B_{12}N_{12}$ and $B_{16}N_{16}$ clusters were studied (Fig. 5). MEP maps indicate that in the adsorption of a drug molecule, clusters are positively charged (blue color with low intensity) while the N atoms are negatively charged (red color with high intensity) and the B atoms are positively charged (blue color) in the B–N bonds of the cluster, therefore, the drug molecule functions as an electron donor and the cluster functions as an electron acceptor owing to a strong adsorption. The semiconducting properties of the $B_{12}N_{12}$ and $B_{16}N_{16}$ nanoclusters with energy gaps of about 6.74 and 6.37 eV, respectively, can be seen in the computed DOS plots from using the B3LYP method, as shown in Fig. 3. Whereas the energy gaps of the $B_{12}N_{12}$ and $B_{16}N_{16}$ clusters were calculated to 4.99 and 4.61 eV with the PBE method, respectively, these represent values significantly smaller than the E_g in the B3LYP method. The energy gap of the $B_{12}N_{12}$ cluster was experimentally computed with the value of 5.1 eV by Oku and coworkers.[35] This result is in agreement with the DFT calculation reported by Baei *et al.*[36] The E_g values of the $B_{12}N_{12}$ and $B_{16}N_{16}$ clusters are about 6.93 and 6.46 eV with the B3PW91 functional, respectively. With the adsorption of 5-AVA molecule in the B3PW91 method, the energy gaps of the $B_{12}N_{12}$ and $B_{16}N_{16}$ clusters are significantly reduced to 5.14 and 5.68 eV, respectively. Whereas the energy gaps of the 5-AVA molecule interacting with the $B_{12}N_{12}$ and $B_{16}N_{16}$ clusters are decreased to 3.12 and 3.56 eV in the PBE method, respectively. We found that the calculations of E_g from both configurations in the PBE method were closer to the results of the theoretical data, as mentioned above by Baei *et al.*[36] The calculations of energy gap obtained by the PBE and B3PW91 methods are significantly smaller than those obtained by the B3LYP method.

The quantum molecular descriptors (QMD) of reactivity in the context of DFT calculations are summarized in Tables 2–5.

When the 5-AVA molecule (NH_2 group) was adsorbed on to the $B_{12}N_{12}$ nanocluster, the hardness values were reduced from 3.37, 3.47, and 2.50 eV in the pristine cluster to 2.49, 2.57, and 1.56 eV in the complexes in the B3LYP, B3PW91, and PBE methods, respectively, which means that the stabilities of the complexes are lower than the pristine clusters.[37,38] The electrophilicity index of the drug molecule interacting with the $B_{12}N_{12}$ cluster was drastically higher, with values from 2.98, 2.94, and 3.91 eV in the pristine cluster to 3.80, 4.08, and 6.55 eV in the complexes in the B3LYP, B3PW91, and PBE methods, respectively, indicating the higher electrophilicity of the molecule, which is greater than its electrophile character (see Tables 1–3). TD-DFT calculations for the 5-AVA drug molecule interacting with the $B_{12}N_{12}$ nanocluster were performed.[39] The details of these calculations are listed in Table 7. According to this Table 7, the 5-AVA drug molecule has two excited states at the wavelengths of 400.01 and 394.01 nm with oscillator strengths (f) of 0.0015 and 0.0069 (in the PBE method), respectively. The transition from HOMO−1 to LUMO is observed with a value of 0.0069 of the oscillator strength and a transition energy of 3.15 eV. Two main transitions for the drug molecule in the B3LYP method were observed at wavelengths of 278.26 and 275.06 nm, with oscillator strengths of 0.0019 and 0.0049, respectively. At λ = 275.06 nm, an electron is transferred from HOMO−1 to LUMO, mainly arising from $\pi \rightarrow \pi^*$ electronic excitations,[40,41] with 0.0049 oscillator strength and a transition energy of 4.51 eV. The B3PW91 method involved two bands at 272.32 and 269.14 nm, with f values of 0.00298 and 0.0033, respectively. At a wavelength of 269.14 nm, electron transfer occurred from HOMO−1 to LUMO, which involved 66% as the main transition. The UV-Vis absorption spectrum of the 5-AVA drug molecule on the BN nanoclusters is shown in Fig. 6, with different basis sets. The UV-Vis absorption spectrum from the PBE method exhibits a strong band at 394.01 nm. However, the B3LYP method shows a band at 275.06 nm, while also the UV-Vis absorption spectrum from the B3PW91 method exhibits a band at 269.14 nm. Tables 2 and 3 present the results, which show the four highest and the four lowest molecular orbital energy levels of the 5-AVA drug molecule on the BN nanoclusters. Note that the HOMO–LUMO gap of the PBE method is relatively smaller than in the other methods.

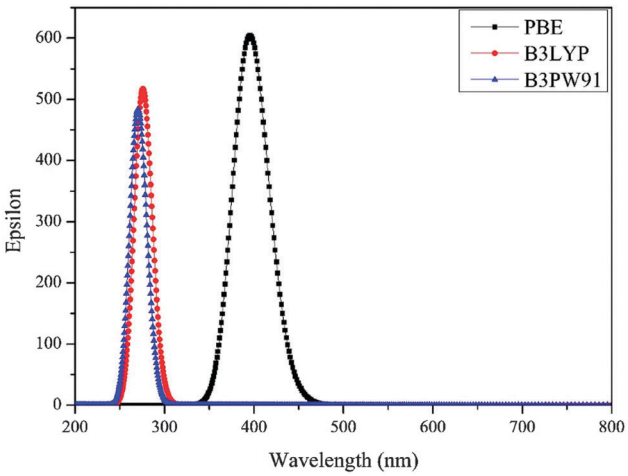

Fig. 6 UV-Vis spectra of the 5-aminolevulinic acid molecule (NH_2 group) on the $B_{12}N_{12}$ nanocages.

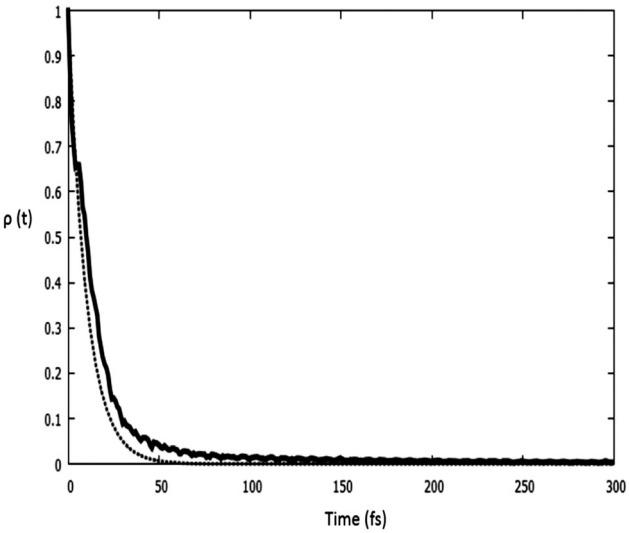

Fig. 7 Time-dependent survival probability in a sensitized $B_{12}N_{12}$ nanocage. The dashed lines are the exponential fitting curves to the two elementary steps for electron transfer in the nanocage.

Table 7 Selected excitation energies (eV, nm), oscillator strength (f), and relative orbital contributions calculated for the most stable configuration

Methods	Energy/ eV	Wavelength/ nm	Oscillator strength (f)	Assignment
B3LYP				
	4.55	278.26	0.0019	H → L (96%)
	4.51	275.06	0.0049	H−10 → L (12%), H−1 → L (82%)
B3PW91				H → L (91%), H−10 → L (4%)
	4.55	272.32	0.0029	H−10 → L (21%), H−1 → L (66%)
	4.61	269.14	0.0033	H−6 → L (3%), H → L (3%)
PBE				
	3.09	400.01	0.0015	H → L (99%)
	3.15	394.01	0.0069	H−1 → L (99%)

Focus was placed on the photoinjection mechanisms from the excited electronic states of the 5-AVA drug molecule with the $B_{12}N_{12}$ nanocluster. Surface sensitization involved the adsorption of a 5-AVA drug molecule to the BN nanocluster surface and the formation of a 5-AVA-BN nanocluster surface compound. Photoexcitation of the surface compound can lead to interfacial electron transfer when there is a suitable energy match between the photoexcited electronic state in the surface compound and the electronic states in the HOMO–LUMO gap of the BN cluster. Injection times as short as a few femtoseconds were investigated for various systems. According to Fig. 7, the time for electron injection in the 5-AVA drug molecule

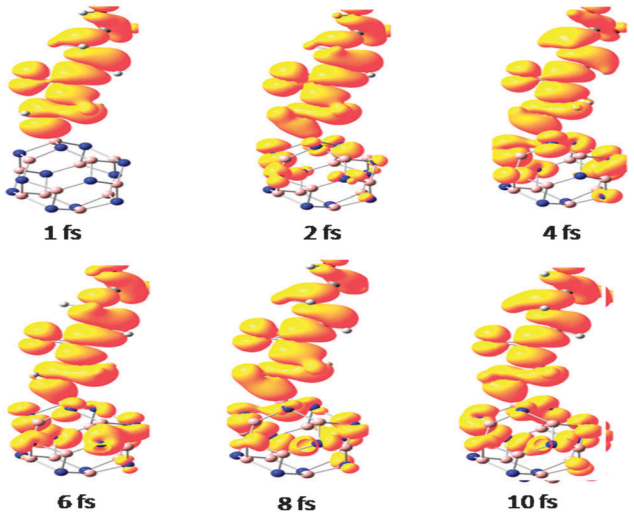

Fig. 8 Evolution of time-dependent charge distribution during the early time relaxation dynamics after instantaneously populating the 5-AVA drug molecule on the $B_{12}N_{12}$ nanocage.

was approximately 10 fs in the $B_{12}N_{12}$ cluster. Fig. 8 shows the evolution of the time-dependent charge distribution during the early time relaxation dynamics after instantaneously populating the 5-AVA-LUMO, including the primary electron-transfer event, within the first 2 fs of dynamics.

4. Concluding remarks

To conclude, we investigated the binding and electronic properties of the covalent functionalization of $B_{12}N_{12}$ and $B_{16}N_{16}$ clusters with 5-aminolevulinic acid drug using DFT calculations. We found that the 5-AVA (NH_2 group) could be drug-loaded and covalently attached to $B_{12}N_{12}$ and $B_{16}N_{16}$ nanoclusters with almost similar binding energies of −2.01 and −1.95 eV in the B3LYP method, respectively, while the apparent results of the B3LYP method are fully different compared with the B3PW91 and PBE methods. The functionalization of the $B_{12}N_{12}$ and $B_{16}N_{16}$ clusters with 5-AVA drug indicate their considerable influence in the electronic properties of the adsorbent. NBO analysis predicted a significant charge transfer from the drug molecule to the adsorbents. We hope our results of the adsorption properties of 5-aminolevulinic acid on $B_{12}N_{12}$ and $B_{16}N_{16}$ nanoclusters can be used as in the adsorbent enhancing delivery of drugs to cancer cells and to support decreased drug interaction with healthy tissue.

Acknowledgements

We would like to thank the Nanotechnology Working Group of Young Researchers and Elite Club of Islamic Azad University, Gorgan Branch, Iran. We should thank the clinical Research Development Unit (CRDU), Sayad Shirazi Hospital, Golestan University of Medical Sciences, Gorgan, Iran.

References

1 S. Mukhopadhyay, R. H. Scheicher, R. Pandey and S. P. Karna, *J. Phys. Chem. Lett.*, 2011, **2**, 2442.
2 S. Mukhopadhyay, S. Gowtham, R. H. Scheicher, R. Pandey and S. P. Karna, *Nanotechnology*, 2010, **21**, 165703.
3 C. Y. Zhi, Y. Bando, C. C. Tang, R. Xie, T. Sekiguchi and D. Golberg, *J. Am. Chem. Soc.*, 2005, **127**, 15996.
4 C. Y. Zhi, Y. Bando, C. C. Tang and D. Golberg, *Phys. Rev. B: Condens. Matter Mater. Phys.*, 2006, **74**, 153413.
5 C. Y. Zhi, Y. Bando, C. C. Tang, Q. Huang and D. Golberg, *J. Mater. Chem.*, 2008, **18**, 3900.
6 D. Golberg, Y. Bando, C. C. Tang and C. Y. Zhi, *Adv. Mater.*, 2007, **19**, 2413.
7 A. Soltani, N. Ahmadian, Y. Kanani, A. Dehno khalaji and H. Mighani, *Appl. Surf. Sci.*, 2012, **258**, 9536.
8 A. Soltani, N. Ahmadian, A. Amirazami, A. Masoodi, E. Tazikeh Lemeski and A. V. Moradi, *Appl. Surf. Sci.*, 2012, **261**, 262.
9 W. L. Wang, Y. Bando, C. Y. Zhi, W. F. Fu, E. G. Wang and D. Golberg, *J. Am. Chem. Soc.*, 2008, **130**, 8144.
10 G. Ciofani, V. Raffa, A. Mencissi and P. Dario, *J. Nanosci. Nanotechnol.*, 2008, **8**, 6223.
11 C. Y. Zhi, J. L. Zhang, Y. Bando, T. Terao, C. C. Tang, H. Kuwahara and D. Golberg, *J. Phys. Chem. C*, 2008, **112**, 17592.
12 G. Ciofani, V. Raffa, A. J. Yu, Y. Chen, Y. Obata, S. Takeoka, A. Mencissi and A. Cuschieri, *Curr. Nanosci.*, 2009, **5**, 33.
13 M. Mirzaei, *Superlattices Microstruct.*, 2013, **57**, 44.
14 E. Erdtman and L. A. Eriksson, *Chem. Phys. Lett.*, 2007, **434**, 101.
15 *Photodynamic Therapy*, ed. T. Patrice, RSC Publishing, 2004.
16 *Photodynamic Therapy with ALA*, ed. R. Baumgartner, R. Pottier, B. Krammer and H. Stepp, RSC Publishing, 2006, and references therein.
17 Q. Peng, T. Warloe, K. Berg, J. Moan, M. Kongshaug, K.-E. Giercksky and J. M. Nesland, *Cancer*, 1997, **79**, 2282.
18 M. D. Ganji, H. Yazdani and A. Mirnejad, *Physica E*, 2010, **42**, 2184.
19 G. Gou, B. Pan and L. Shi, *ACS Nano*, 2010, **4**, 1313.
20 S. Y. Xie, W. Wang, K. A. S. Fernando, X. Wang, Y. Lin and Y. P. Sun, *Chem. Commun.*, 2005, 3670.
21 J.-X. Zhao and Y.-h. Ding, *Diamond Relat. Mater.*, 2010, **19**, 1073.
22 C. Y. Zhi, Y. Bando, W. L. Wang, C. C. Tang, H. Kuwahara and D. Golberg, *Chem. – Asian J.*, 2007, **2**, 1581.
23 M. Kia, M. Golzar, K. Mahjoub and A. Soltani, *Superlattices Microstruct.*, 2013, **62**, 251.
24 M. W. Schmidt, K. K. Baldridge, J. A. Boatz, S. T. Elbert, M. S. Gordon, J. H. Jensen, S. Koseki and N. Matsunaga, *et al.*, *J. Comput. Chem.*, 1993, **14**, 1347.
25 A. Ahmadi Peyghan, N. Hadipour and Z. Bagheri, *J. Phys. Chem. C*, 2013, **117**, 2427.
26 J. Beheshtian, A. Ahmadi Peyghan and M. Noei, *Sens. Actuators, B*, 2013, **181**, 829.
27 S. F. Rastegar, A. Ahmadi Peyghan and N. L. Hadipour, *Appl. Surf. Sci.*, 2013, **265**, 412.

28 A. Bahrami, S. Yourdkhani, M. D. Esrafili and N. L. Hadipour, *Sens. Actuators, B*, 2014, **191**, 457.
29 J. P. Perdew, K. Burke and M. Ernzerhof, *Phys. Rev. Lett.*, 1996, **77**, 3865.
30 A. D. J. Becke, *J. Chem. Phys.*, 1993, **98**, 5648.
31 (*a*) R. G. Pearson, *Proc. Natl. Acad. Sci. U. S. A.*, 1986, **83**, 8440; (*b*) A. Soltani, M. T. Baei, A. S. Ghasemi, E. Tazikeh Lemeski and K. Hosseni Amirabadi, *Superlattices Microstruct.*, 2014, **75**, 564.
32 A. Soltani, M. T. Baei, E. Tazikeh Lemeski and A. A. Pahlevani, *Superlattices Microstruct.*, 2014, **75**, 716.
33 E. C. Anota and G. H. Cocoletzi, *Physica E*, 2014, **56**, 134.
34 N. Saikia, S. K. Pati and R. C. Deka, *Appl. Nanosci.*, 2012, **2**, 389.
35 T. Oku, A. Nishiwaki and I. Narita, *Sci. Technol. Adv. Mater.*, 2004, **5**, 635.
36 M. T. Baei, *Comput. Theor. Chem.*, 2013, **1024**, 28.
37 N. Saikia and R. C. Deka, *Comput. Theor. Chem.*, 2011, **964**, 257.
38 Z. B. Nojini, F. Yavari and S. Bagherifar, *J. Mol. Liq.*, 2012, **166**, 53.
39 H. Ullah, A.-u.-H. Ali Shah, S. Bilal and K. Ayub, *J. Phys. Chem. C*, 2013, **117**, 23701.
40 N. Sanna, G. Chillemi, L. Gontrani, A. Grandi, G. Mancini, S. Castelli, G. Zagotto, C. Zazza, V. Barone and A. Desideri, *J. Phys. Chem. B*, 2009, **113**, 5369.
41 A. Soltani and M. Bezi Javan, *RSC Adv.*, 2015, **5**, 90621.

